

High-photosensitive resin for super-resolution direct-laser-writing based on photoinhibited polymerization

Yaoyu Cao,¹ Zongsong Gan,¹ Baohua Jia,¹ Richard A. Evans,² and Min Gu^{1,*}

¹Centre for Micro-Photonics and Centre for Ultrahigh-bandwidth Devices for Optical Systems (CUDOS), Faculty of Engineering and Industrial Science, Swinburne University of Technology, P.O. Box 218 Hawthorn, VIC 3122, Australia

²CSIRO Materials Science and Engineering, Bag 10, Clayton South MDC, Victoria 3169, Australia
*mgu@swin.edu.au

Abstract: An ethoxylated bis-phenol-A dimethacrylate based photoresin BPE-100 of relatively high photosensitivity and modulus is used for the creation of sub-50 nm features. This is achieved by using the direct laser writing technique based on the single-photon photoinhibited polymerization. The super-resolution feature is realized by overlapping two laser beams of different wavelengths to enable the wavelength-controlled activation of photoinitiating and photoinhibiting processes in the polymerization. The increased photosensitivity of the photoresin promotes a fast curing speed and enhances the photopolymerization efficiency. Using the photoresin BPE-100, we achieve 40 nm dots for the first time in the super-resolution fabrication technique based on the photoinhibited polymerization, and a minimum linewidth of 130 nm. The influence of the power of the inhibiting laser and the exposure time on the feature size is studied and the results agree well with the prediction obtained from a simulation based on a non-steady-state kinetic model.

©2011 Optical Society of America

OCIS codes: (220.4241) Nanostructure fabrication; (220.4610) Optical fabrication; (140.3450) Laser-induced chemistry; (160.5335) Photosensitive materials; (160.5470) Polymers.

References and links

1. J. W. Perry, B. H. Cumpston, S. P. Ananthavel, S. Barlow, D. L. Dyer, J. E. Ehrlich, L. L. Erskine, A. A. Heikal, S. M. Kuebler, I.-Y. S. Lee, D. McCord-Maughon, J. Qin, H. Röckel, M. Rumi, X.-L. Wu, and S. R. Marder, "Two-photon polymerization initiators for three-dimensional optical data storage and microfabrication," *Nature* **398**(6722), 51–54 (1999).
2. M. Deubel, G. von Freymann, M. Wegener, S. Pereira, K. Busch, and C. M. Soukoulis, "Direct laser writing of three-dimensional photonic-crystal templates for telecommunications," *Nat. Mater.* **3**(7), 444–447 (2004).
3. K. Choi, J. W. M. Chon, M. Gu, N. Malic, and R. A. Evans, "Low-distortion holographic data storage media using free-radical ring-opening polymerization," *Adv. Funct. Mater.* **19**(22), 3560–3566 (2009).
4. L. Li, E. Gershgoren, G. Kumi, W. Y. Chen, P. T. Ho, W. N. Herman, and J. T. Fourkas, "High-performance microring resonators fabricated with multiphoton absorption polymerization," *Adv. Mater. (Deerfield Beach Fla.)* **20**(19), 3668–3671 (2008).
5. S. Maruo, A. Takaura, and Y. Saito, "Optically driven micropump with a twin spiral microrotor," *Opt. Express* **17**(21), 18525–18532 (2009).
6. Z. Xiong, X. Z. Dong, W. Q. Chen, and X. M. Duan, "Fast solvent-driven micropump fabricated by two-photon microfabrication," *Appl. Phys., A Mater. Sci. Process.* **93**(2), 447–452 (2008).
7. T. F. Scott, B. A. Kowalski, A. C. Sullivan, C. N. Bowman, and R. R. McLeod, "Two-color single-photon photoinitiation and photoinhibition for subdiffraction photolithography," *Science* **324**(5929), 913–917 (2009).
8. H. B. Sun, K. Takada, M. S. Kim, K. S. Lee, and S. Kawata, "Scaling laws of voxels in two-photon photopolymerization nanofabrication," *Appl. Phys. Lett.* **83**(6), 1104–1106 (2003).
9. M. Z. Sun, Y. Li, H. B. Cui, H. Yang, and Q. H. Gong, "Minimum spacing between suspended nanorods determined by stiction during two-photon polymerization," *Appl. Phys., A Mater. Sci. Process.* **100**(1), 177–180 (2010).
10. C. Decker and K. Moussa, "Real-time kinetic-study of laser-induced polymerization," *Macromolecules* **22**(12), 4455–4462 (1989).
11. G. Odian, *Principles of Polymerization*, Fourth Edition (John Wiley & Sons, Inc.: Hoboken, New Jersey 2004).

12. H. Q. Hou, J. G. Jiang, and M. X. Ding, "Ester-type precursor of polyimide and photosensitivity," *Eur. Polym. J.* **35**(11), 1993–2000 (1999).
13. J. Serbin, A. Ovsianikov, and B. Chichkov, "Fabrication of woodpile structures by two-photon polymerization and investigation of their optical properties," *Opt. Express* **12**(21), 5221–5228 (2004).
14. I. V. Khudyakov, W. S. Fox, and M. B. Purvis, "Photopolymerization of vinyl acrylate studied by photodsc," *Ind. Eng. Chem. Res.* **40**(14), 3092–3097 (2001).
15. L. H. Nguyen, M. Straub, and M. Gu, "Acrylate-based photopolymer for two-photon microfabrication and photonic applications," *Adv. Funct. Mater.* **15**(2), 209–216 (2005).
16. M. Trujillo-Lemon, J. H. Ge, H. Lu, J. Tanaka, and J. W. Stansbury, "Dimethacrylate derivatives of dimer acid," *J. Polym. Sci., Part A: Polym. Chem.* **44**(12), 3921–3929 (2006).
17. S. H. Wu, M. Straub, and M. Gu, "Single-monomer acrylate-based resin for three-dimensional photonic crystal fabrication," *Polymer (Guildf.)* **46**(23), 10246–10255 (2005).
18. T. A. Pham, P. Kim, M. Kwak, K. Y. Suh, and D. P. Kim, "Inorganic polymer photoresist for direct ceramic patterning by photolithography," *Chem. Commun. (Camb.)* **39**, 4021–4023 (2007).
19. Z. S. Gan, Y. Y. Cao, B. H. Jia, and M. Gu, "Dynamic modeling of photoinhibited photopolymerization for superresolution photolithography," under preparation.
20. E. T. Denisov, T. G. Denisova, and T. S. Pokidova, *Handbook of free radical initiators* (John Wiley & Sons, Inc.: Hoboken, New Jersey 2004).
21. M. R. Gleeson and J. T. Sheridan, "Nonlocal photopolymerization kinetics including multiple termination mechanisms and dark reactions. Part i. Modeling," *J. Opt. Soc. Am. B* **26**(9), 1736–1745 (2009).
22. M. Gu, *Advanced optical imaging theory* (Springer: Verlag Berlin Heidelberg 2000).

1. Introduction

In the past decade, the direct laser writing technique employing photo-initiated polymerization has attracted enormous research interests due to its broad applications in microfluidic devices, microelectromechanics systems, photonics and optical information storage and processing [1–6]. However, fabrication resolution limited by the diffraction nature of light in the direct laser writing technique represents a great challenge for achieving functional structures and devices, such as metamaterials and photonic crystals operating in the visible wavelength region. Interest in the development of a fast and inexpensive super-resolution fabrication method, which is capable of generating deep-subwavelength feature size with robust mechanical strength, is rapidly increasing.

Recently, a breakthrough in nanofabrication has been achieved by using the photoinhibited polymerization process, in which a diffraction-limit-free fabrication was demonstrated [7]. In this method, two laser beams of two colors were overlapped at the focal spot. One laser beam (initiating beam) was used for starting the polymerization, while the other (inhibiting beam) used to suppress the polymerization by generating a polymerization inhibiting species. As the exposure zone of the inhibiting beam was modulated to a doughnut shape, a diffraction-limit-free polymerization volume could be generated in the centre of the exposed region. This approach neatly combined the production of a smaller photo-active voxel and the prevention of dark polymerization [8], which is of great promise to realize super-resolution fabrication. Based on this method, Scott and associates demonstrated 65 nm dots with a single photon fabrication process. However, the photoresin used in the reported work is of a slow curing speed and a low modulus after gelation [9], which could bring unexpected loss in resolution and therefore imposes a great challenge for reaching the full resolution capacity of the photoinhibited polymerization.

In photopolymerization, for a given polymerizable group, low curing speed indicates low quantum yields related to the photoinitiation and chain propagation [10]. For a given light absorber—a initiator or a photosensitizer and a polymerizable group, an increase of the photosensitivity of the photoresin, where the photosensitivity can be expressed as the amount of photoenergy that is required to react half of the monomers, can enhance the quantum yield of the photoinduction and photopolymerization triggered by the photons absorbed. In this regard, the population of photons required to achieve the polymerization threshold is decreased, which potentially leads to a reduced light scattering. As a result, the polymerization caused by the detrimental factor is minimized leading to a smaller polymerization voxel. After the polymerization, the solvent washing process for removing the unsolidified monomers can bring stress changes on the gelled structure. For a given stress change, the high modulus of the gelled structure leads a low strain [11]. In this case, the high

modulus and crosslinking can enhance the resistance of the photoresin to the developing solvent, which prevents the distortion and size variance of the structure. Therefore, the photoresin of high photosensitivity and high modulus after the gelation is essential for a super-resolution fabrication.

In this letter, we demonstrate that a methacrylate-based monomer can be used to increase the fabrication speed and reduce the feature size in the fabrication based on the single-photon photoinhibited polymerization process. The monomer of high viscosity increases the photosensitivity of the photoresin [12] and enables a fast polymerization speed. The high modulus offers rigid strength [9] for a sharp edge of the patterns. The minimum feature size is reduced to 40 nm by the irradiation of inhibition light, which is 1/12 of the wavelength of the initiating laser used in the fabrication.

2. Experimental

2.1 Materials and sample preparation

The bifunctional monomer NK Ester BPE-100 (2.2 Bis[4-(Methacryloxy Ethoxy)Phenyl]Propane) and TEGDMA (Triethyleneglycol Dimethacrylate), which have two reactive methacrylate groups per molecule, were purchased from Shin-Nakamura Chemical Co. Ltd, Japan. To prevent spontaneous polymerization, the normal inhibitor in the monomers was retained and the monomers were used as purchased. The photoinitiator camphorquinone (CQ), coinitiator ethyl 4-(dimethylamino)benzoate (EDAB), photoinhibitor tetraethylthiuram disulfide were provided by Aldrich, USA. The solvent acetone, ethanol and isopropanol were AR grade.

To prepare the photoresin, the photoinitiator, coinitiator and photoinhibitor in the photoresin were firstly dissolved in acetone and then mixed with BPE-100. The mixture was kept in the oven at the temperature of 50°C for 12 hrs to remove acetone. At last, the photoresin used for the fabrication was consisted of photoinitiator of 1 wt%, coinitiator of 0.5 wt% and photoinhibitor of 3.5 wt%, respectively, stored in dark refrigerator. Samples used for direct laser writing were prepared by spin-coating a drop of photoresin to achieve evenly spread area and then sandwiching the photoresin between two coverslips separated by a 40 μ m thick sticky-tape spacer [13]. The coverslip was used as purchased without surface treatments.

2.2 Photodifferential Scanning Calorimetry (Photo-DSC)

A TA-Instruments Photo-DSC was used to characterize the polymerization of the photoresin BPE-100 and the photoresin TEGDMA [14, 15]. A high pressure mercury arc lamp with the output power of 100W was used to irradiate samples through two light-guided fibres, emitting light of the spectra region from 250 nm-650 nm. The photoresin BPE-100 used for heat characterization was consisted of CQ, EDAB and BPE-100 with the content of 1 wt%, 0.5 wt% and 98.5 wt%, respectively. The photoresin TEGDMA was formulated similar to the photoresin BPE-100, where the monomer BPE-100 was replaced by TEGDMA. The exposure intensity of the light was fixed at 60 mW/cm².

2.3 Fabrication

A CW mode 375 nm inhibiting laser (Coherent-cube, USA) for inhibiting polymerization was modulated to a Laguerre-Gaussian mode by a planar vortex phase plate (RPC Photonics Inc. USA). A CW mode 488 nm initiating laser (Melles Griot Laser 643-RYB, USA) of a Gaussian mode was used to initiate the polymerization. The inhibiting laser beam was circularly polarized and the initiating laser beam was linearly polarized. The inhibiting laser beam and the initiating laser beam were combined by a dichroic mirror before entering a 100 \times objective of NA = 1.4 (Olympus). Quantum dot clusters, emitting light of the wavelength region from 550 nm- 650 nm, was used as a position indicator to align these two beams. After fabrication, the coverslip containing the gelated structure was rinsed in the pure isopropanol for 2 min and then in the pure ethanol for 30 sec.

2.4 Scanning electron microscope (SEM)

A ZEISS Supra 40 VP Field Emission Scanning Electron Microscope, operating at 3KV, was used to image the polymer patterns fabricated by laser direct writing. Before the measurement, the sample was coated with a gold layer with the thickness of 3-4 nm.

3. Result and discussion

When free radical polymerization is used for fabricating micro/nano-structures, the performance of the monomers becomes significant. In general, a monomer of high viscosity can shorten the exposure time and improve the photosensitivity [9]. A monomer of good mechanical stability can resist the variance of the size and the shape during fabrication and post-processing. Specially, in the case of photoinhibited polymerization, it should be noticed that increasing viscosity is able to increase the polymerization rate by suppressing the bimolecular termination reaction on one hand [12]. But on the other hand, the inhibition efficiency is decreased due to the reduced mobility of the inhibitor. Thus, the viscosity of the photoresin has to be carefully controlled to provide enough photosensitivity without decreasing the inhibition efficiency. To satisfy the criteria of photoinhibited polymerization, the monomer of NK Ester BPE-100 was introduced into the photoresin. It was an ethoxylated bis-phenol-A dimethacrylate with an average of 2.6 ethyleneglycol units per molecule. The viscosity of BPE-100 was 1000 mPa·s, much higher than the photoresin TEGDMA (triethyleneglycol dimethacrylate) that was used in the previous work, where the viscosity was 8 mPa·s [16]. Moreover, the aromatic groups in the BPE-100 can provide higher modulus [17] to enhance the mechanical stability to resist the distortion during solvent washing.

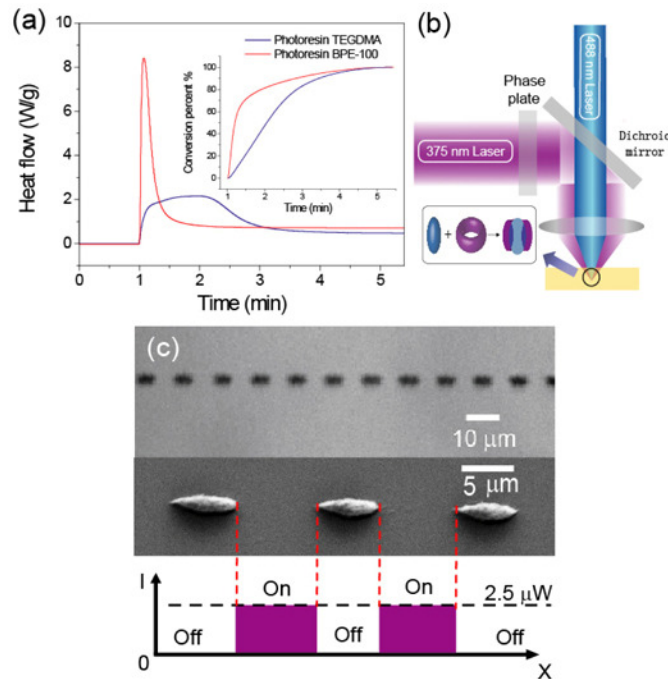


Fig. 1. (a) The heat flow against the exposure time of the photoresin TEGDMA and BPE-100 measured by the Photo-DSC (the inset is the relevant conversion percent against exposure time). (b) Scheme of the optical setup for photoinhibited polymerization. (c) Optical microscopic and SEM images of the dashed line fabricated in the photoresin BPE-100 by the irradiation of an inhibiting laser beam at intervals. The violet columns represent the sections of the line exposed to the inhibiting laser. The status of the exposure of the inhibiting laser switches the polymerization.

The polymerization processes of the photoresin BPE-100 and TEGDMA were characterized by the photoDSC (TA-Instruments Q1000) at the temperature of 20°C. For a given temperature and an irradiation density, the peak of the heat flow during the polymerization is proportional to the photosensitivity of the photoresin. Figure 1(a) shows the heat flow against the exposure time for the photoresin BPE-100 and TEGDMA. The maximum heat flow of the photoresin TEGDMA is 2.1 W/g. In comparison, the exothermal peak of BPE-100 is at 8.4 W/g, which indicates the photoresin BPE-100 has an enhanced photopolymerization kinetic [18]. According to the profile of the conversion percent, 50% percent conversion was reached within 1 min in the photoresin TEGDMA and 0.2 min in the photoresin BPE-100. This result suggests that the photosensitivity of the Photoresin BPE-100 is five times higher than that of the photoresin TEGDMA. The heat flow peak of BPE-100 is much sharper, implying a faster initial polymerization speed and thus a shorter exposure time is required to achieve the threshold.

To investigate the behavior of the photoresin BPE-100 in photoinhibited polymerization, a single-photon fabrication setup was developed, as show in Fig. 1(b). A 488 nm laser (initiating beam) for activating initiator radicals and another 375 nm laser (inhibiting beam) for exciting inhibitor radicals were combined by a dichroic mirror, and then focused with an objective of NA = 1.4. The photoresin BPE-100 was scanned at a speed of 2 $\mu\text{m/s}$ by the 488 nm initiating laser at the power of 200 nW. During the scanning, the 375 nm inhibiting laser with a Gaussian profile was focused to the same position to inhibit the polymerization. We found that the polymerization in the region under the inhibiting laser irradiation was completely halted when the power of the laser reached 2.5 μW , as shown in Fig. 1(c) in the interval between the line segments. The fabricated polymer segments have sharp boundaries manifesting the photoresin BPE-100 of high photoinhibiting efficiency for the photoinhibited polymerization.

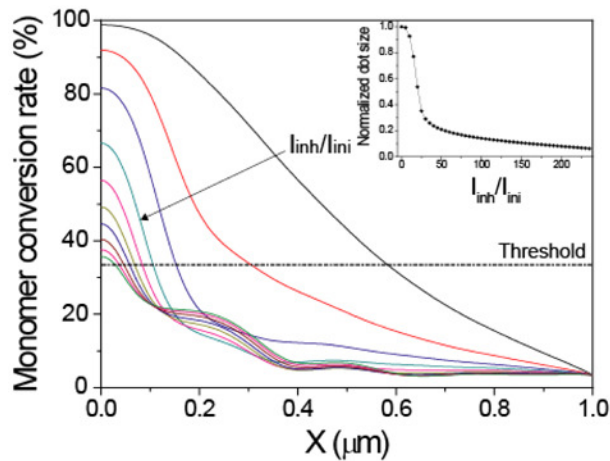


Fig. 2. Simulation results of the conversion rate of monomer are plotted along the transverse direction at different levels of the irradiation intensity of the inhibiting laser. The arrow indicates the direction of increasing the ratio of the irradiation intensity of the inhibiting laser to the initiating laser. The inset is the normalized dot size as a function of the ratio of the irradiation intensity of the inhibiting laser to the initiating laser. In the calculation, the absorption cross section of initiator and the inhibitor is $2.1 \times 10^{-21} \text{cm}^2$ and $5.9 \times 10^{-21} \text{cm}^2$ respectively. The rate constants for the initiation caused by the photoinitiator (CQ), the termination caused by the photoinhibitor (TED), and the initiation caused by the photoinhibitor (TED) are $3 \times 10^7 \text{cm}^3 \text{mol}^{-1} \text{s}^{-1}$, $1.2 \times 10^8 \text{cm}^3 \text{mol}^{-1} \text{s}^{-1}$ and $3 \times 10^5 \text{cm}^3 \text{mol}^{-1} \text{s}^{-1}$, respectively. The rate constant for the polymerization is $2 \times 10^6 \text{cm}^3 \text{mol}^{-1} \text{s}^{-1}$. The rate constant for the chain termination is $4 \times 10^7 \text{cm}^3 \text{mol}^{-1} \text{s}^{-1}$. The diffusion constant of initiator/inhibitor radicals is $0.25 \mu\text{m}^2/\text{s}$ and the diffusion constant of chain-initiating radicals is $0.05 \mu\text{m}^2/\text{s}$. These values were based on the literatures [11, 20, and 21] and estimated from the fits to the experimental data.

To predict the theoretical limit of the photoinhibited photopolymerization with the photoresin BPE-100, we built up a non-steady-state kinetic model to simulate the variation of the achievable feature size by changing the power ratio between the initiating beam and the inhibiting beam [19]. This model involves the dynamic process of the light absorption, the radical generation, initiation, inhibition and polymerization, which could calculate time-dependent conversion rate variation of the monomer under certain light irradiation. We considered the recombination of free radicals caused by the confining effect, photo-inhibitor induce polymerization, the diffusion of the photo-initiator radicals and the photo-inhibitor radicals and the changes of the polymerization kinetic constants caused by the increased viscosity within the focus spot [20, 21]. Figure 2 shows the plot of the conversion rate of the monomers in the focal plane for an exposure time of 0.7 s, where the exposure time was estimated according to the fabrication parameters used for fabricating the line shown in Fig. 1(c). The conversion rate of the monomers around the focal spot can be determined, given the distribution of the light intensity at the focal spot by the vectorial-Debye theory [22]. In the calculation, a Laguerre-Gaussian beam was used for the inhibiting beam. It reveals that increasing the irradiation intensity ratio of the inhibiting laser to the initiating beam leads to a significant suppression of the conversion rate in the exposed region of the inhibiting laser, which implies an improved fabrication resolution can be achieved. As the monomer of BPE-100 is a bifunctional molecule, the threshold of the polymerization is the conversion rate of 33% [11], which determines the feature size of the dots. According to the conversion rate plot, the change of the normalized feature size of the dots reveals two gradients with the increase of the irradiation intensity ratio of the inhibiting laser to initiating laser, as shown in the inset of Fig. 2. When the irradiation intensity ratio of the inhibiting beam to the initiating beam increases up to 25, the gradients of the variance of the feature size of the dots are reduced with the increase of the intensity of the inhibiting laser, indicating a reduced inhibition strength of the inhibitor radicals.

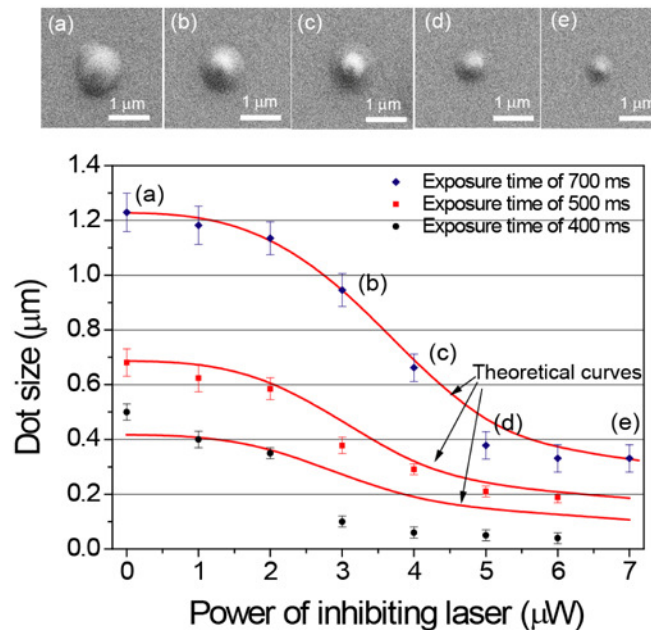


Fig. 3. The dot sizes are plotted as a function of the power of the inhibiting laser in the photoresin BPE-100. The dots were fabricated under the exposure of the initiating laser of the power of 200 nW at the exposure time of 0.7 s. The SEM images are corresponding to the dots fabricated under the exposure of different power of the inhibiting laser. The red curves are the simulated results with the exposure time of 0.7 s, 0.5 s and 0.4 s, respectively, and the exposure of the initiating laser of power of 200 nW.

The theoretical predication on reduced feature size was confirmed by the dot fabrication at different power levels of the inhibiting laser. In experiment, the dots were fabricated with a fixed initiating laser power of 200 nW at a constant exposure time of 0.7 s. As shown in Fig. 3, it is clearly that the dot size decreased from 1200 to 330 nm when the power of the inhibiting laser increased. These results agree remarkably well with the numerical simulation and the deviation between the experimental value and simulation data is less than 25%. As the power of the inhibiting laser increased from 0 to 5 μW , the dot size decreased to 1/3 of that fabricated without the inhibiting laser. On the contrary, the dot size only decreased by 13% when the power of the inhibiting laser was further increased to 7 μW , which implies that the inhibition effect approaches saturation. In addition, we recognized that the size reduction percent of 75% in the photoresin BPE-100 by increasing the power of the inhibiting laser is smaller than that of 87% revealed in the photoresin TEGDMA [7]. This can be explained by the decreased inhibition efficiency in the photoresin BPE-100 caused by high viscosity induced low mobility of the inhibitors. Moreover, when the exposure time is changed to 0.5 s and 0.4 s, the curves represent similar tendencies to that obtained at the exposure time of 0.7 s. For the exposure time of 0.4 s, the experimental values became smaller than the calculated result, when the power of the inhibiting laser was larger than 2 μW . This is attributed to the low conversion percent of the monomer in the exposure region, which might cause partially polymerization, resulting in the deviation from the experiment. From these results, we can conclude that the dynamic processes in the fabrication control the super-resolution fabrication.

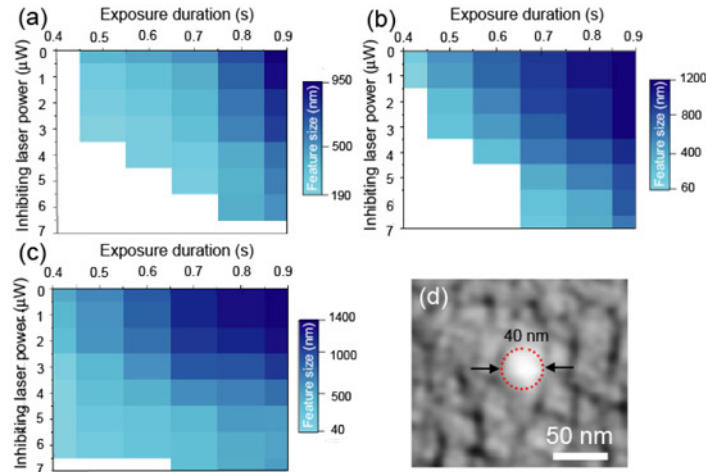


Fig. 4. The experiment results of the dots fabricated with different exposure conditions. The dot sizes are plotted as a function of the power of the inhibiting laser and the exposure time. The exposure power of the initiating laser is (a) 130 nW, (b) 160 nW and (c) 200 nW. (d) is the SEM image of the dot fabricated under the irradiation of the initiating laser of 200 nW and the inhibiting laser of 6 μW at the exposure time of 0.4 s.

To optimize the fabrication condition, the measured feature sizes of dots were plotted against the inhibiting laser power and the exposure time at different power levels of the initiating laser, as shown in Fig. 4. It clearly reveals that the short exposure time can produce smaller dots. For a longer exposure time from 0.5 s to 0.9 s, the minimum feature sizes are all above 100 nm. For example, under the exposure of the initiating laser power of 160 nW and the exposure time of 0.6 s, the minimum feature size is 310 nm. Because the long exposure time complicates the fabrication process, such as the polymerization initiated by the scattered light, the fabrication is not just dominated by the ratio of the input power of the inhibiting laser to the power of the initiating laser. As a consequence, the feature size is difficult to reduce by only changing the power of the inhibiting laser. Moreover, the reproducibility of the fabrication is also decreased. For a lower power of the initiating laser of 130 nW, the

minimum feature size cannot be reduced below 190 nm. These results suggest that the fabrication of nanodots can only be realized in a limited region of the fabrication condition, where the higher power of the initiating laser and the shorter exposure time are desirable. With the initiating laser of 200 nW and the inhibiting laser of 6 μ W, a dot of 40 nm was produced, which is around 1/12 of the wavelength of the initiating laser.

With the resin BPE-100, we also investigated the line fabrication based on the photoinhibited polymerization. In principle, the fabrication of lines is different from the fabrication of dots where the centre of the dots is not irradiated by the inhibiting laser. During scanning a straight line, all of the points on the scanning routine were under the exposure of the inhibiting laser, which leads to unavoidable change in the conversion rate profile of the lines. Accordingly, the irradiation intensity of the inhibiting laser has to be well controlled to minimize the feature size of lines and maintain the continuity. Figure 5(a) shows a homogeneous line scanned at a speed of 3 μ m/s and the power of the initiating laser of 200 nW. The sharp edge of the line also indicates good mechanical strength of the photoresin that can resist the distortion after the solvent washing. Figures 5(b)-(e) show the linewidth variation against the power of the inhibiting laser. It clearly depicts that increase of the inhibiting laser power from 0 μ W to 2 μ W can reduce the linewidth from 400 nm to 130 nm.

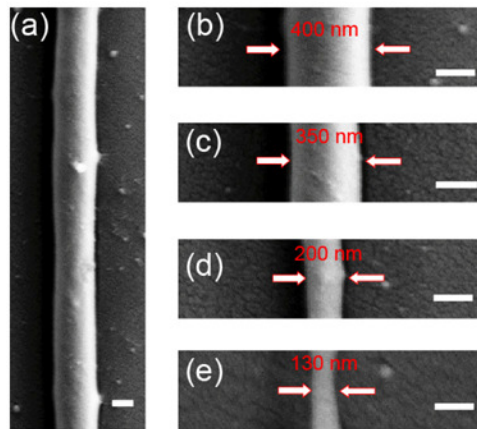


Fig. 5. (a) is the SEM image of a line fabricated at a fixed scanning speed of 3 μ m/s, under the exposure of initiating laser of constant power of 200 nW. (b)-(e) are the lines fabricated with different power levels of the inhibiting laser: for (b) 0 μ W, (c) 1.0 μ W, (d) 1.5 μ W and (e) 2.0 μ W, at the scanning speed of 3 μ m/s, under the irradiation of initiating laser of 200 nW. The scale bar represents 200 nm.

4. Conclusion

In conclusion, the photoresin NK Ester BPE-100 of high photosensitivity and mechanical stability has been developed to improve the fabrication based on the single-photon photoinhibited polymerization. A CW mode inhibiting laser beam of 375 nm was used to inhibit the photopolymerization. The high inhibition efficiency of the photoresin allows the inhibiting laser to easily terminate the polymerization. A kinetic model has been developed to simulate the function of the power of the inhibiting laser in the fabrication of dots, which reveals the inhibiting laser can significantly reduce the dot size. Experimentally, we have demonstrated a dot of 40 nm, which is 1/12 of the initiating laser wavelength. We found that the nanodots are presented only at a short exposure time and a relatively high power level of the initiating laser. Moreover, straight lines with the reduced linewidth of 70% have been fabricated under the exposure of the inhibiting laser, compared with a 400 nm line fabricated without the inhibiting laser. These findings reveal that the development of the photoresin can provide more opportunities for single-photon direct-laser-writing technique to fully explore the capacity of the photoinhibited polymerization. Tuning the diffusion ability of the inhibitor

to increase the inhibition efficiency of the photoresin and applying multifunctional monomers to enhance polymer crosslinking networks could potentially bring a further improvement to achieve the feature size in a sub10 nm scale.

Acknowledgment

This work is produced with the assistance of the Australian Research Council (ARC) under the Centres of Excellence Program. CUDOS (the Centre for Ultrahigh-bandwidth Devices for Optical Systems) is an ARC Centre of Excellence. Min Gu thanks the Australian Research Council for its support through the Laureate Fellowship scheme (FL100100099). Baohua Jia is supported by ARC Australian Postdoctoral Fellowship (APD) grant DP0987006